Electronic Supplementary Material (ESI) for Dalton Transactions

Supporting Information

Charge-distribution-related regioisomerism of photoresponsive metal-organic polymeric chains

Jian-Ke Sun,[a,b] Peng Wang,[a,b] Cheng Chen,[a] Xue-Jun Zhou,[a,b] Li-Ming Wu,[a] Yong-Fan Zhang[c] and Jie Zhang*[a]

[a] *State Key Laboratory of Structural Chemistry, Fujian Institute of Research on the Structure of Matter, Chinese Academy of Sciences, Fuzhou, Fujian 350002, P. R. China. E-mail: zhangjie@fjirsm.ac.cn; Fax: (+86) 591-83710051*
[b] *Graduate School of Chinese Academy of Sciences, Beijing, 100039, P. R. China*
[c] *Department of Chemistry,Fuzhou University, Fuzhou, Fujian 350002, P. R. China*

****

This file includes:

Section 1. Synthesis of ligands

Section 2. Additional characterization data and structural figures

Section 1. Synthesis of ligands

The ligand H_2**L1**·Cl_2 was synthesized with following method: according to the route shown in Scheme S1.

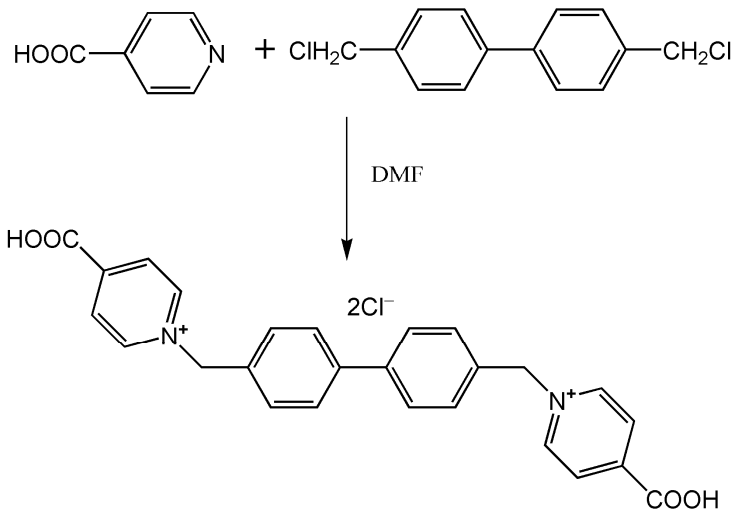

Scheme S1 Schematic representation of the synthesis procedure of H_2**L1**·Cl_2.

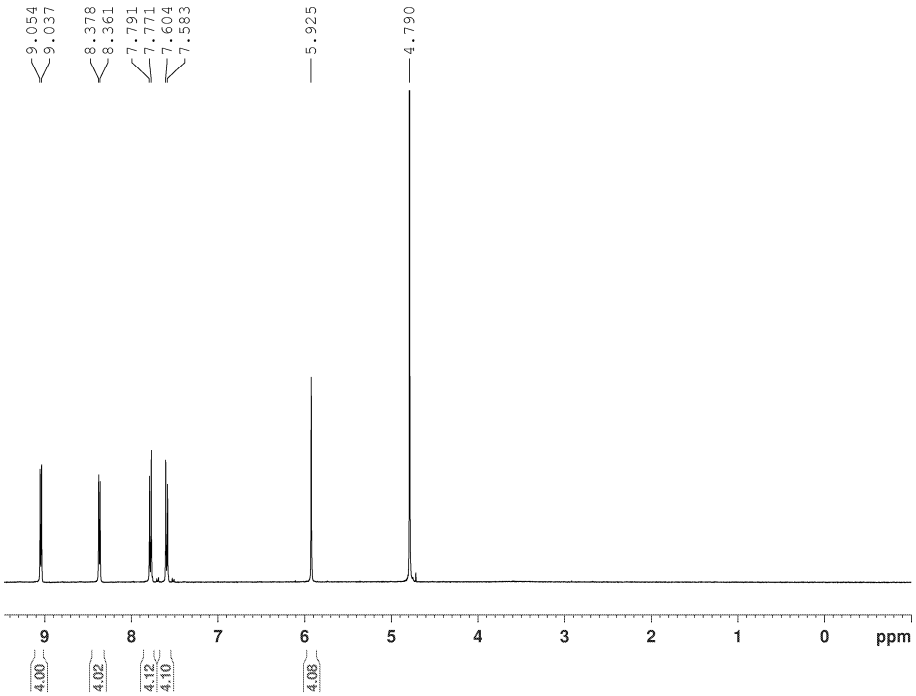

^{1}H NMR (400 MHz, D_2O) for H_2**L1**·Cl_2**.** δ 9.05 (d, J = 6.8 Hz, 4H), 8.37 (d, J = 6.7 Hz, 4H), 7.78 (d, J = 8.3 Hz, 4H), 7.59 (d, J = 8.3 Hz, 4H), 5.92 (s, 4H).

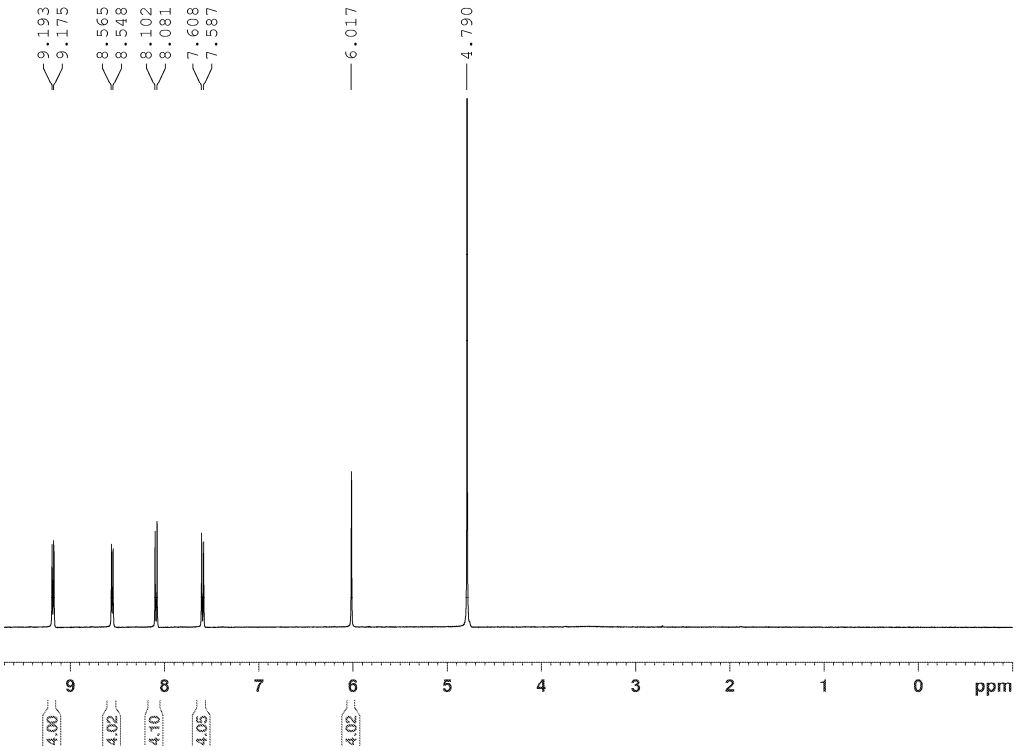

^{1}H NMR (400 MHz, D_2O) for H_2**L2**·Cl_2**.** δ 9.18 (d, *J* = 7.0 Hz, 4H), 8.56 (d, *J* = 7.0 Hz, 4H), 8.09 (d, *J* = 8.4 Hz, 4H), 7.60 (d, *J* = 8.4 Hz, 4H), 6.02 (s, 4H).

Section 2. Additional characterization data and structural figures

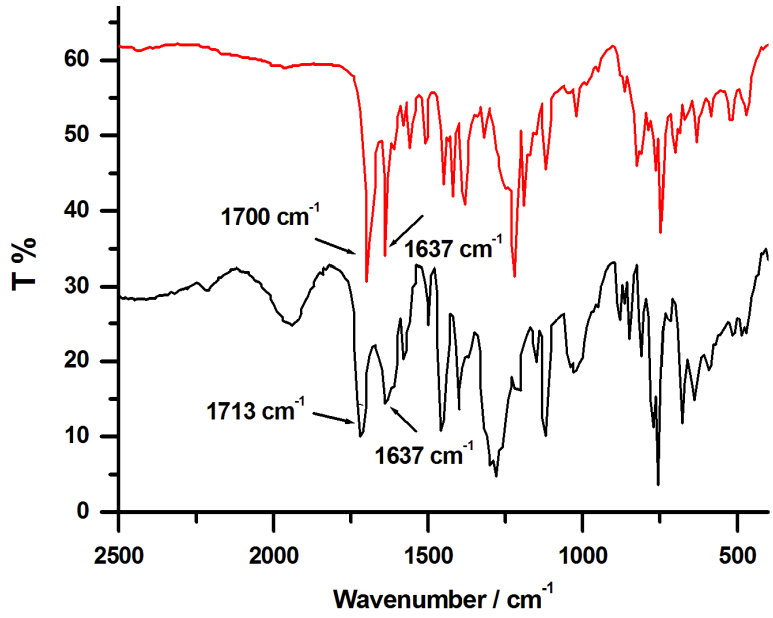

Fig. S1 IR spectra of H_2**L1**·Cl_2 (black) and H_2**L2**·Cl_2 (red). The asymmetrical C=O stretch of the carboxylic group appears at 1713 cm^{-1} for H_2**L1**·Cl_2, and 1700 cm^{-1} for H_2**L2**·Cl_2, respectively. The strong bands around 1637 cm^{-1} are characteristic for the C=N and C=C stretching vibrations of the pyridinium groups.

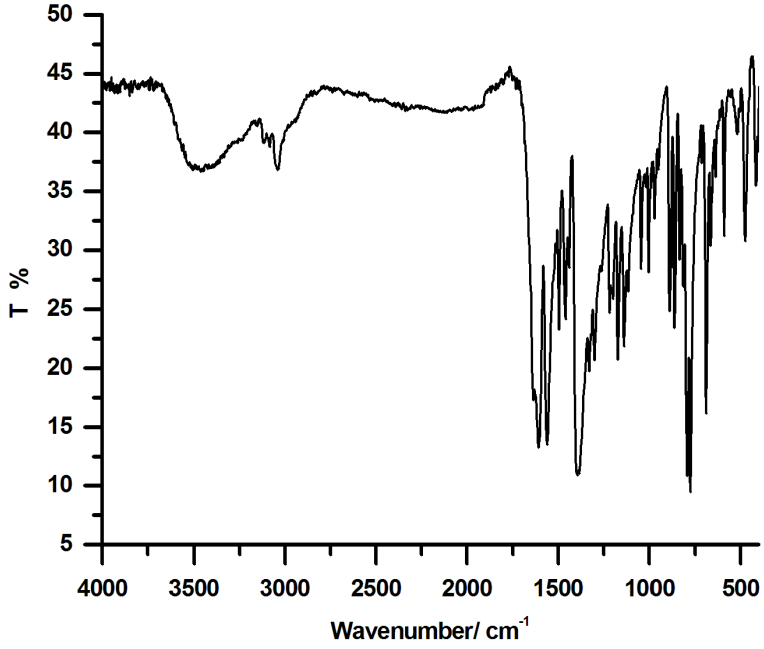

Fig. S2 IR spectrum of complex **1**.

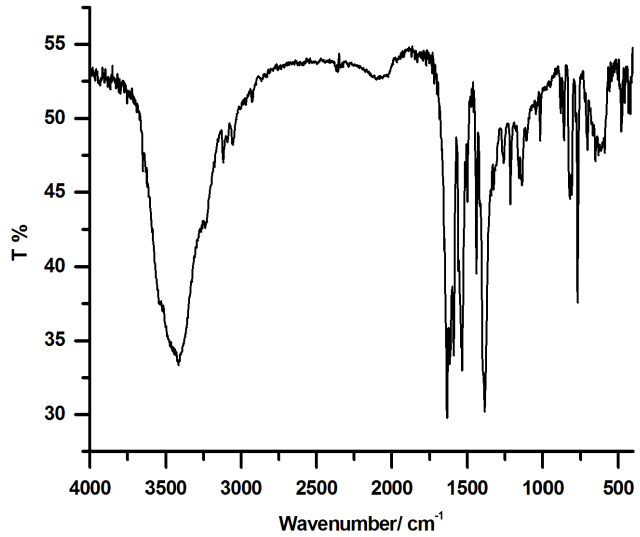

Fig. S3 IR spectrum of complex **2**.

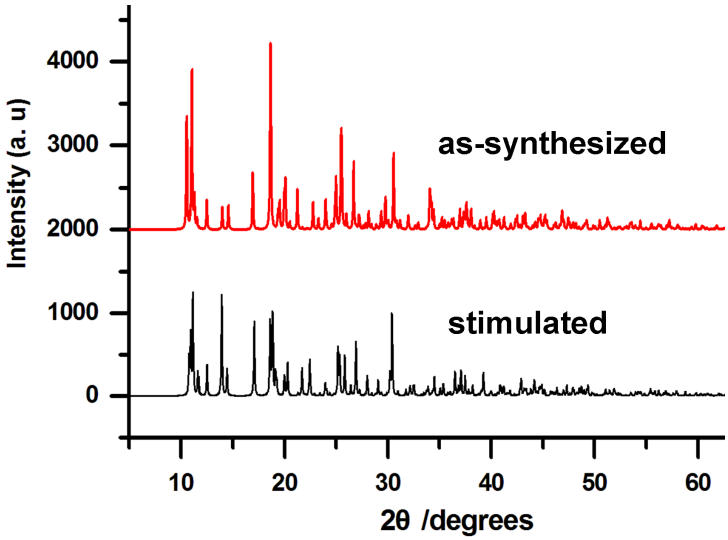

Fig. S4 X-ray powder-diffraction patterns for simulated and as-synthesized **1.**

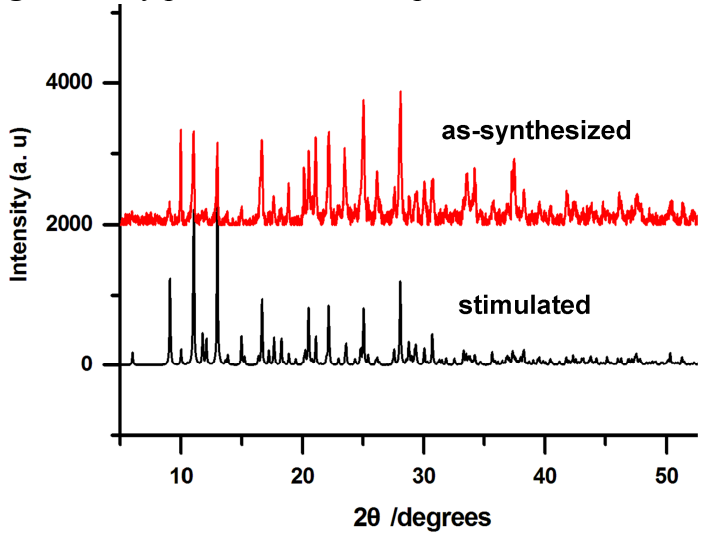

Fig. S5 X-ray powder-diffraction patterns for simulated and as-synthesized **2.**

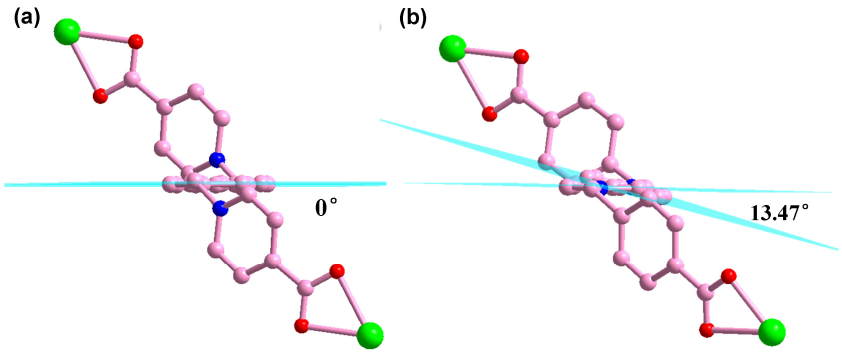

Fig. S6 The tilt angles of biphenyl ring (a) in **1** and bipyridinium rings (b) in **2**.

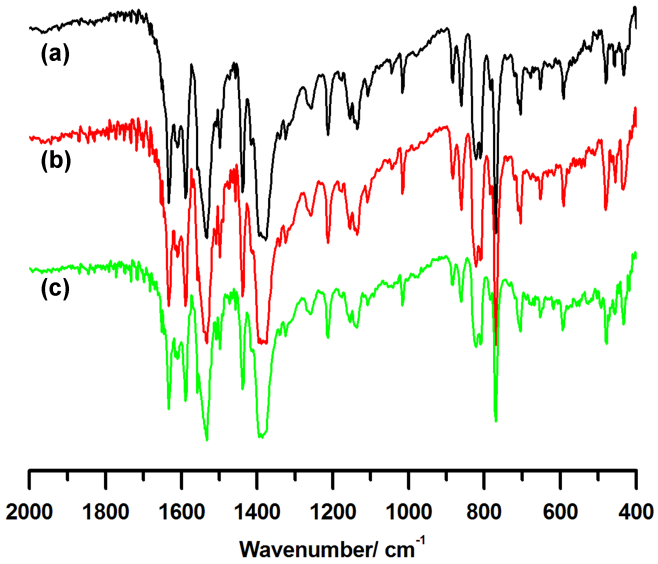

Fig. S7 IR spectra of complex **2** before and after photoirradiation, (a) original sample, (b) after photoirradiation for 30 min, (c) after repeating the color development and bleaching for five cycles. No obvious spectral changes demonstrate that complex **2** remains stable after several color-bleach cycles.

Fig. S8 ESR spectrum of **2** upon photoirradiation (g = 2.0018).

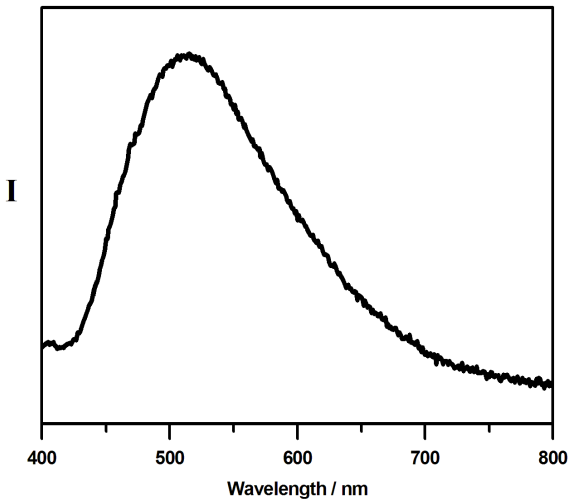

Fig. S9 The luminescence spectrum of ligand H_2**L1**·Cl_2 (λ_{ex} = 370 nm).

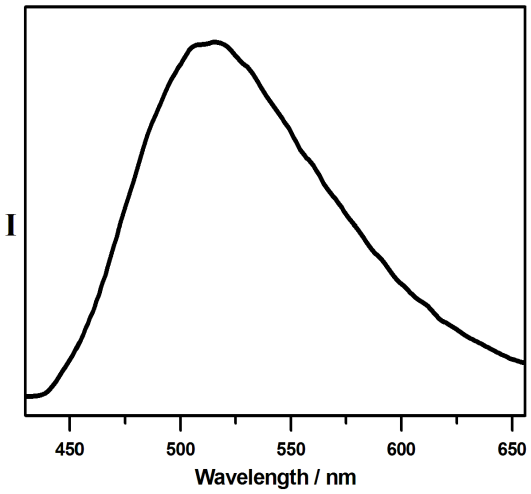

Fig. S10 The luminescence spectrum of ligand H_2**L2**·Cl_2 (λ_{ex} = 390 nm).

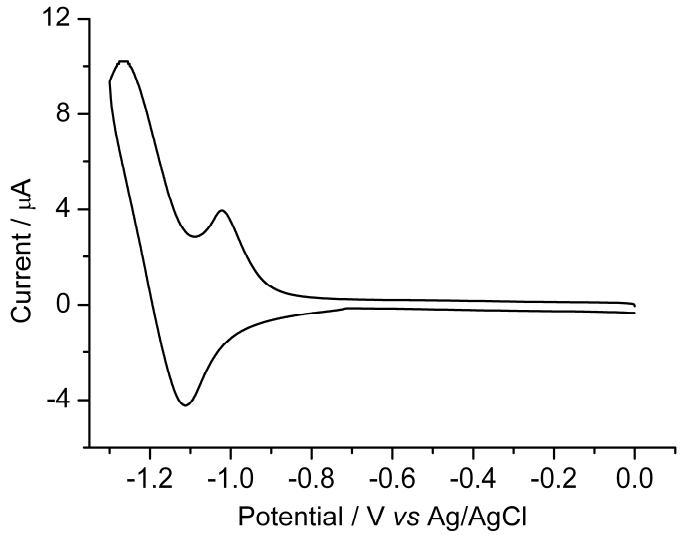

Fig. S11 Cyclic voltammogram of **L1** with 50 mV s^{-1} scan rate in DMSO.

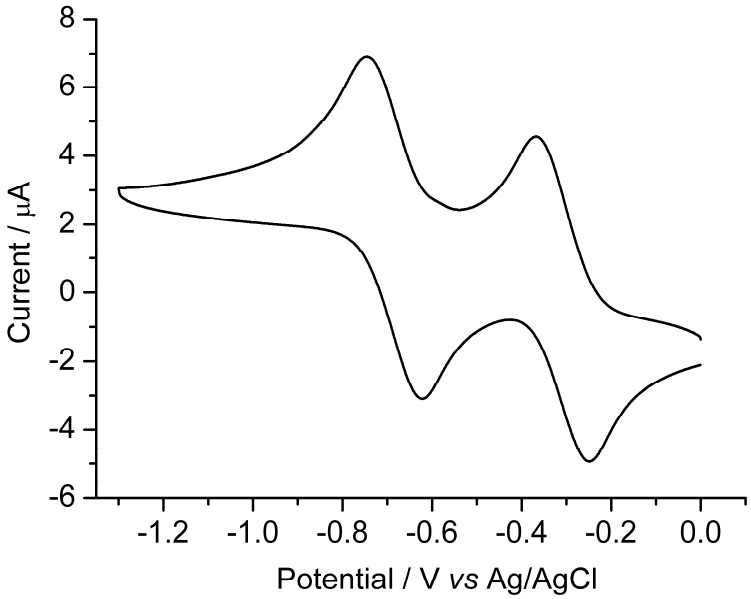

Fig. S12 Cyclic voltammogram of **L2** with 50 mV s^{-1} scan rate in DMSO.

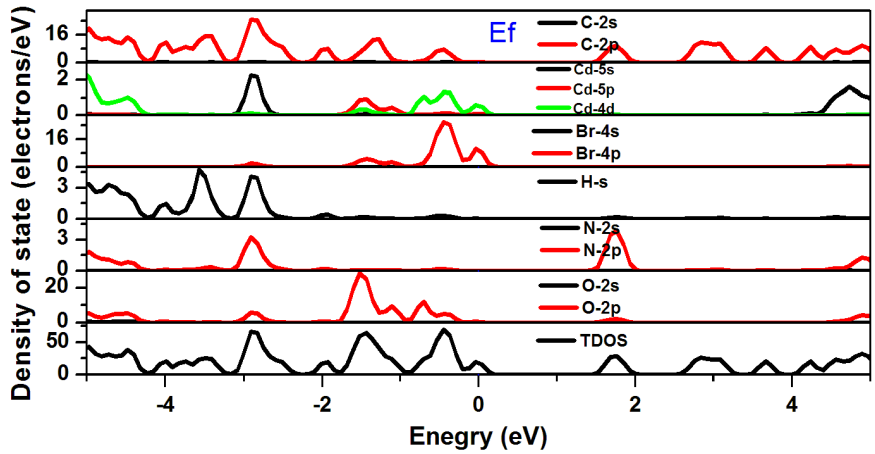

Fig. S13 Total and partial density of states for **1**. (The Fermi level is set at 0 eV.)

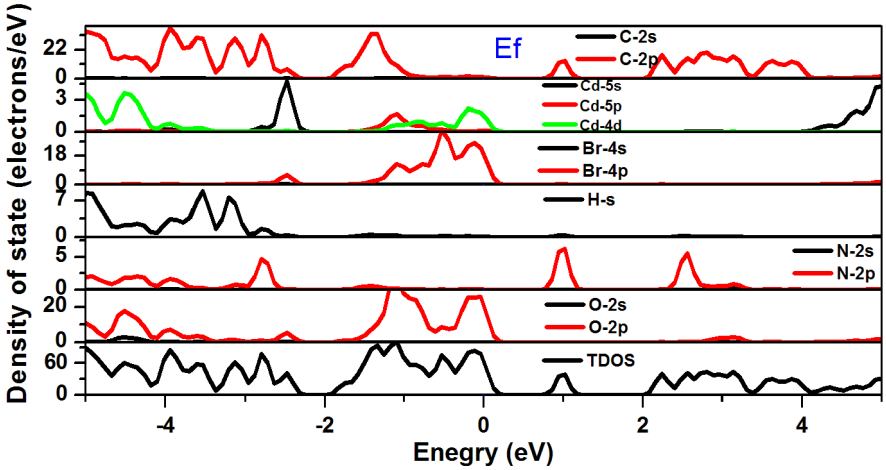

Fig. S14 Total and partial density of states for **2**. (The Fermi level is set at 0 eV.)

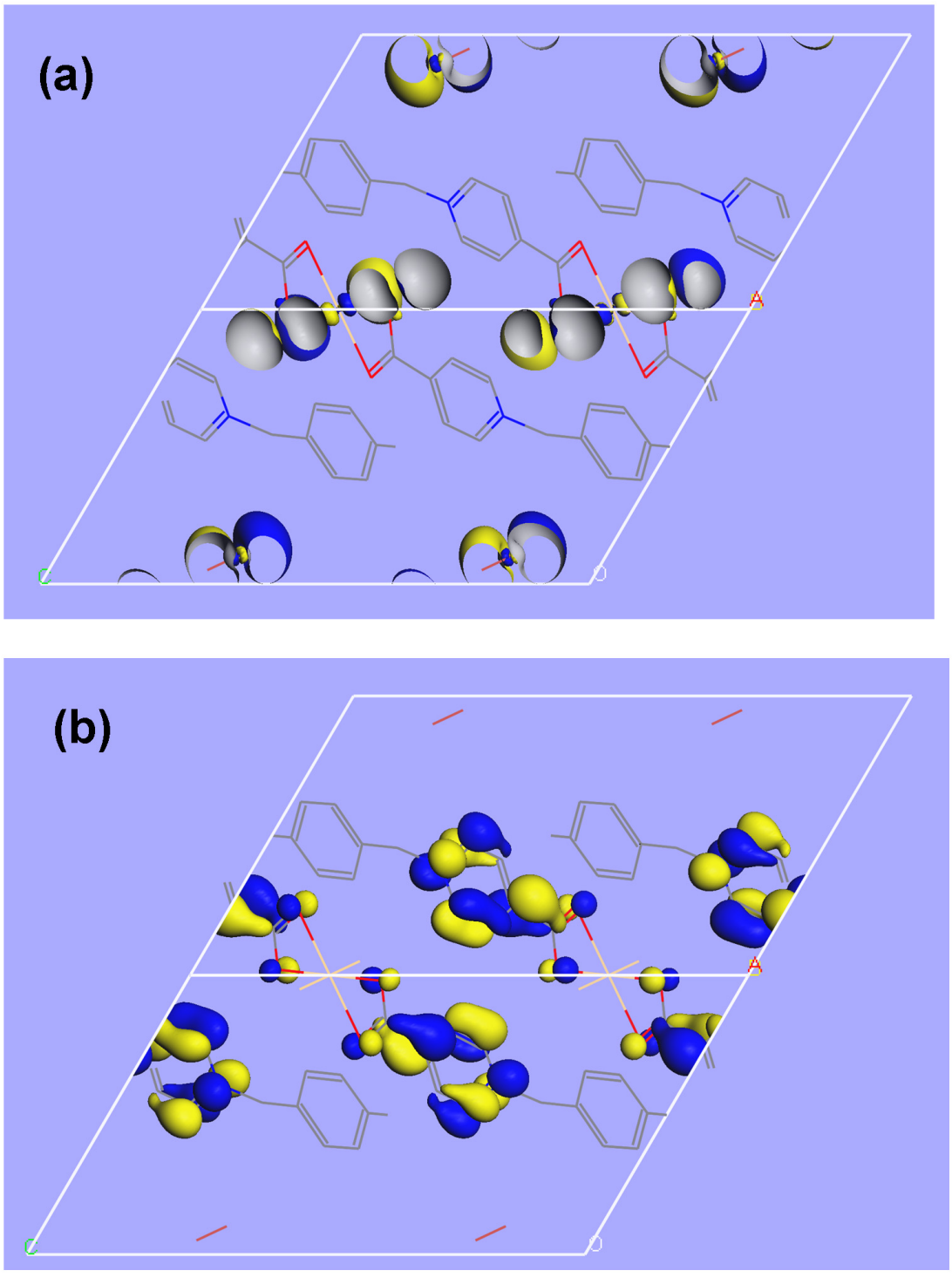

Fig. S15. Electron-density distribution of the highest occupied (a) and lowest unoccupied (b) frontier orbitals for **1** in a unit cell.

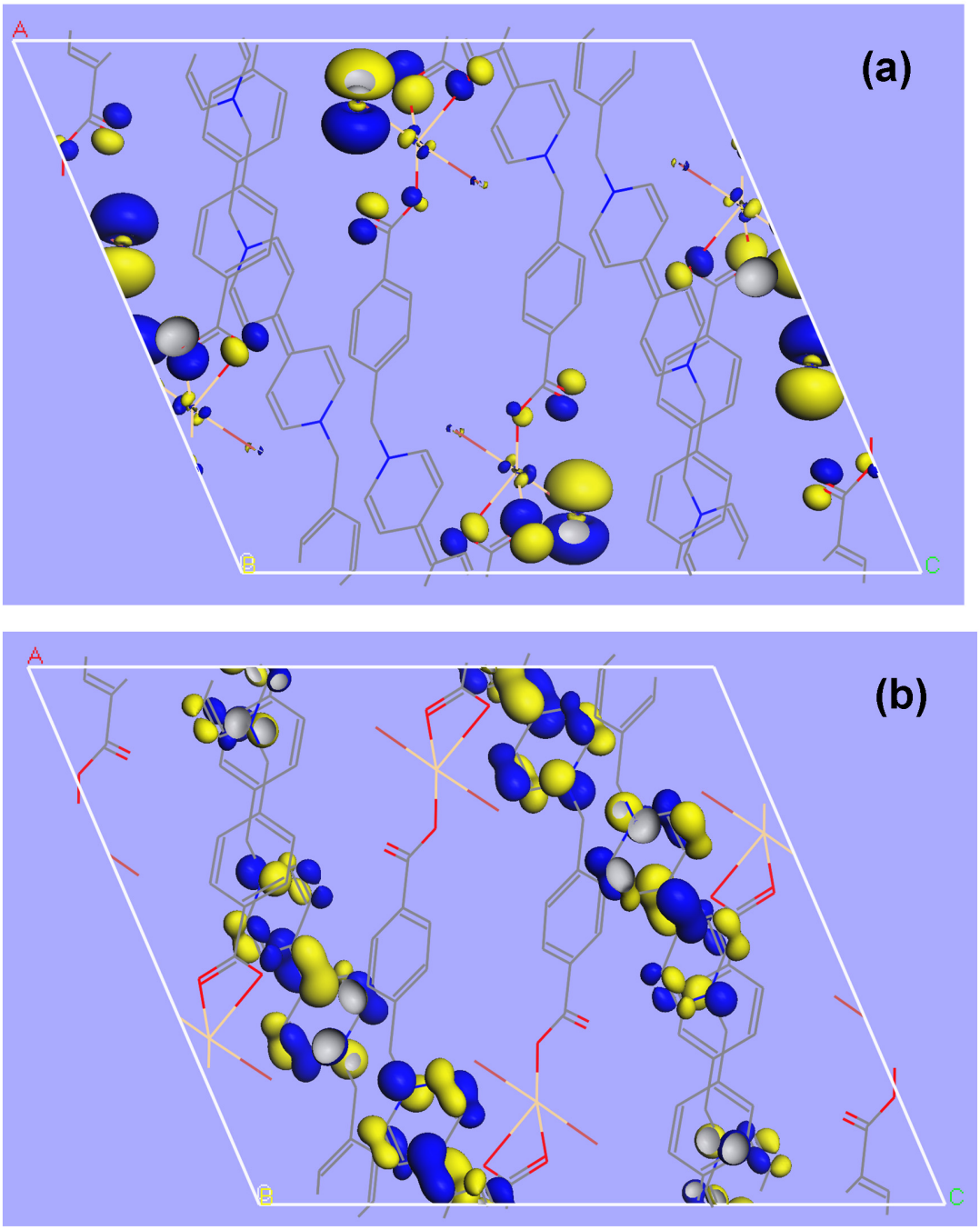

Fig. S16 Electron-density distribution of the highest occupied (a) and lowest unoccupied (b) frontier orbitals for **2** in a unit cell.

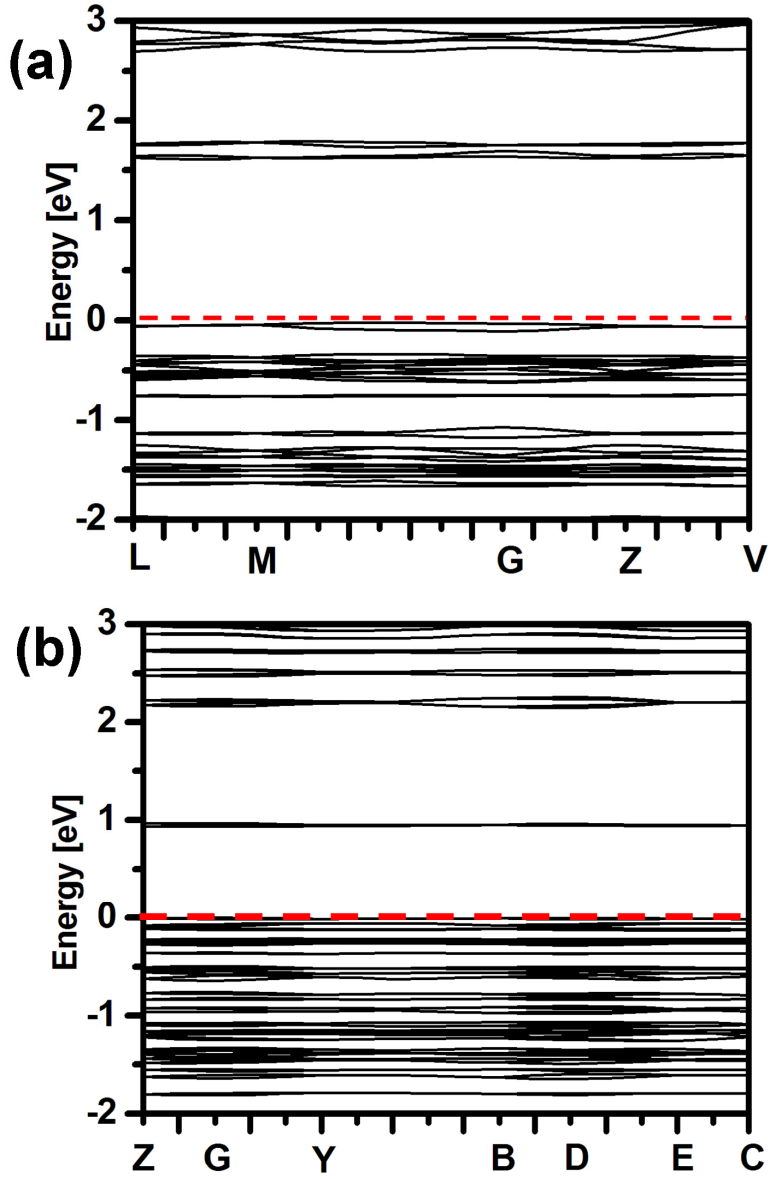

Fig. S17 Band structures of **1**(a) and **2**(b), The Fermi levels are located on 0 eV (dashed lines).

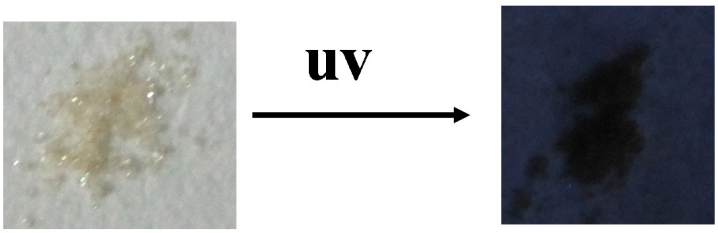

Fig. S18 No luminescence can be observed for **2** under UV lamp (λ = 365 nm)

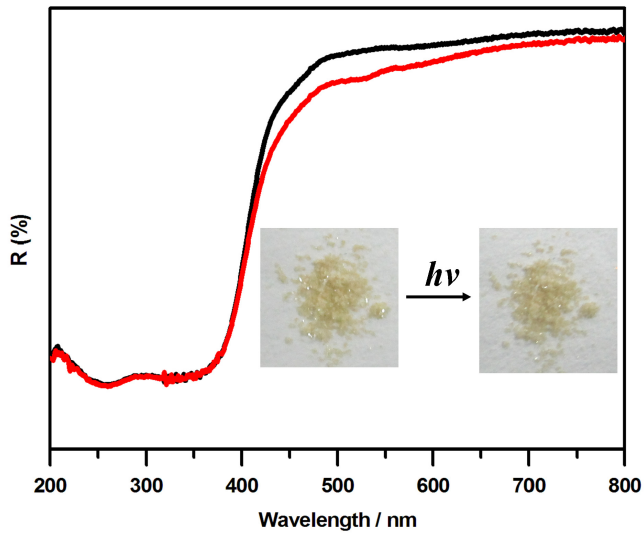

Fig. S19 The UV-vis diffuse reflectance spectra of **1** before (black) and after (red) irradiated with Xenon lamp. No significant spectral change is consistent with the photographic images of the polycrystalline samples upon irradiation shown in the inset.

Table S1. Decomposed HVB (Highest Valence Band) characters (in % per unit cell) for two complexes

	Cd		C		N	O	Br
	p	d	s	p	p	p	p
1	0.62	4.68	0	3.03	0	4.19	86.34
2	0.74	3.69	0	1.43	0	34.92	56.77

Table S2. Decomposed LCB (Lowest Conduction Band) characters (in % per unit cell) for two complexes

	H	C		N	O	Br
	s	s	p	p	p	p
1	0.61	0.12	60.37	23.20	12.21	0.73
2	1.54	0	62.99	29.95	0.05	1.50